Results in Geochemistry 5 (2021) 100012

Contents lists available at ScienceDirect

Results in Geochemistry

journal homepage: www.elsevier.com/locate/ringeo

The potential for a continuous 10Be record measured on ice chips from a borehole

Long Nguyen[a,*], Chiara I. Paleari[a], Stefanie Müller[a], Marcus Christl[b], Florian Mekhaldi[a,c], Philip Gautschi[b], Robert Mulvaney[c], Julius Rix[c], Raimund Muscheler[a]

[a] Department of Geology, Faculty of Science, Lund University, Sölvegatan 12, S-223 62 Lund, Sweden
[b] Laboratory of Ion Beam Physics, ETH Zurich, CH-8093 Zurich, Switzerland
[c] British Antarctic Survey, Cambridge CB3 0ET, UK

ARTICLE INFO

Keywords:
AMS
Sample preparation
Beryllium 10
Ice core
Solar activity

ABSTRACT

Ice cores are excellent archives for obtaining long and continuous ^{10}Be records. However, traditional ice core ^{10}Be measurements required a lot of ice (0.5–1kg) and often needed to be connected to a large and costly ice core project. These reasons have been the factors limiting the number and variety of ^{10}Be projects and data. In this paper, we show measurements of ^{10}Be on small samples (~45g) of continuous auger ice chips from a borehole at Little Dome C (LDC), East Antarctica. The sample preparation method for ^{10}Be accelerator mass spectrometry (AMS) was tested and optimized using test samples (~50g) including well-mixed surface ice chips from the LDC site, snow collected in Lund (Sweden) and frozen Milli-Q water. The results show that our small ice samples should be processed without ion exchange filtration of the melt water and cleaning the subsequent $Be(OH)_2$ precipitate. In addition, co-precipitating Be with Fe led to more reproducible measurement currents and offer the potential for higher efficiency and precision via longer measurement time. We applied the established preparation method to measure ^{10}Be on 76 samples of the auger ice chips. The resulting ^{10}Be concentration record for the period from 1354 to 1950 CE agrees well with the ^{10}Be concentration in a South Pole ice core and the global ^{14}C production rate and thus reflects well the atmospheric production signal of ^{10}Be. We also observed insignificant mixing among the ice chip samples during the process of drilling and retrieving the ice. Therefore, the new ice chip samples are promising for assessing the long-term changes in ^{10}Be deposition at different ice core sites. A wide application of this novel ice chip samples will increase the variety of ^{10}Be records which will help to improve the assessment of long-term solar and geomagnetic shielding of galactic cosmic rays.

1. Introduction

^{10}Be is a long-lived radionuclide ($T_{1/2}$=1.387±0.012 Ma, (Korschinek et al., 2010)) produced mainly from cosmic ray-induced spallation of nitrogen and oxygen atoms in the atmosphere. ^{10}Be has a wide range of applications ranging from reconstructing solar activity and the Earth's magnetic shielding of galactic cosmic rays, to studying atmospheric mixing, hydrological processes and dating of geological archives (Muscheler et al., 2016; Zheng et al., 2021; Mekhaldi et al., 2020; Adolphi and Muscheler, 2016; Alley, 1995). For most of these applications, the samples (e.g. from rocks, sediments or ice cores) contain only a tiny amount of ^{10}Be, i.e. in the range of 10^5 to 10^8 atoms per sample (Christl and Kubik, 2013). Such low concentrations in natural samples result in isotopic ^{10}Be/^{9}Be ratios typically in the range from 10^{-7} to 10^{-11} (Lachner et al., 2020; Christl et al., 2010). The natural ^{10}Be/^{9}Be ratio is usually diluted to 10^{-12} to 10^{-15} after the addition of a defined amount of stable ^{9}Be, the so-called carrier, required in many cases for sample handling and measurement. Since the 1980's ^{10}Be has been routinely measured with Accelerator mass spectrometry (AMS) systems, which can reach detection limits that are many orders of magnitude lower than regular mass spectrometers (Kutschera, 2013; Synal, 2013).

Ice cores are excellent natural archives that can provide well-preserved and detailed ^{10}Be records. However, significant resources are required to drill and collect a deep ice core which then, in most cases, has to be distributed among many different laboratories for analysing a set of other proxies such as stable water isotopes, impurities and trapped gases. Because of the naturally low concentration of ^{10}Be, a

Abbreviation: AMS, Accelerator mass spectrometry; ANOVA, Analysis of variance; EPICA Dome C, EDC; IEC, Ion exchange column; LDC, Little Dome C; RAID, Rapid Access Isotope Drill.

* Corresponding author at: Department of Geology, Lund University Faculty of Science: Lunds Universitet Naturvetenskapliga fakulteten, Sölvegatan 12, S-223 62, Lund, Skåne, Sweden.

E-mail address: hoang_long.nguyen@geol.lu.se (L. Nguyen).

https://doi.org/10.1016/j.ringeo.2021.100012
Received 9 July 2021; Received in revised form 30 October 2021; Accepted 1 November 2021

large amount of ice is often required for ^{10}Be measurement. This has been the limiting factor for many ^{10}Be projects, especially for the achievable temporal resolution. For example, ^{10}Be measurements for Greenland Ice Core Project (GRIP) required from 0.5 kg to 1 kg of ice per sample for AMS measurement (Yiou et al., 1997). Therefore, new inventive ways to obtain ice core samples for ^{10}Be-analysis can allow projects that were not possible up to now. Increasing the ^{10}Be data base is important to improve estimates of the global production rate signal that is linked to solar and geomagnetic shielding since each ice core site has its local influences and weather noise (Muscheler et al., 2016).

The targeted temporal resolution of ^{10}Be ice samples for most applications, except for studies of seasonal atmospheric mixing, is usually one year per sample or longer depending on the focus of the study. Mixing or dating uncertainties in the range of months and even up to several years might not be problematic depending on the focus of the study. Therefore, a fully intact and undisturbed ice core, which preserves the stratigraphy well, might not be necessary for ^{10}Be AMS measurements. Recently, ^{10}Be has been measured in ice core drill chips, that are by-products resulting from continuously scraping-off ice with rotating knives of an ice core drill, from a cold Alpine glacier (Zipf et al., 2016). The resulting ^{10}Be concentrations of the ice chip samples with a temporal resolution of roughly one year agreed well with the ^{10}Be concentration of the ice core samples despite some possible mixing of drill chips. This demonstrated the possibility of utilising ice core drill chips for ^{10}Be measurements from an ice core project, and consequently saving precious ice core samples. The British Antarctic Survey has developed a new drilling method, the so called Rapid Access Isotope Drill (RAID), that is based on an auger enclosed in a barrel that collects ice chips instead of recovering a fully intact ice core (Rix et al., 2019). Ice samples can be recovered extremely fast with this method (the drill design called for around 461 m of ice to be drilled in Antarctica in 104 h) and are suitable for stable water isotope and ^{10}Be analysis. This opens up the prospect of fast recovery of samples for a continuous ^{10}Be record not necessarily connected to a large and costly ice core project. The drill chips are recovered in a barrel during drilling with the stratigraphy mostly intact but some mixing of drill chips is expected leading to some smoothing of the proxy signal versus depth/time.

Here we explore the suitability of ice chips collected via the RAID method for ^{10}Be-analysis. Several test samples with similar properties were prepared and analysed to evaluate a practical way (in terms of ice-saving and cost-efficiency) to process the new ice chip samples for routine AMS analysis. We aim to assess the quality of the very small samples and the results from the ice chips drilled with RAID.

2. Material and methods

2.1. Samples

2.1.1. New drill chip samples

The ice chips studied here were recovered using the RAID method at a site called Little Dome C (LDC), at a distance of approximately 40 km from the Dome Concordia station (75°05′59″S, 123°19′56″E) in East Antarctica. A total depth of 461 m was drilled in austral summer 2017/2018. We investigated 76 samples of ice chips from this drill campaign which cover a depth of 33.5 m from the surface. The weight of each sample was 45 g, with the exception of one smaller sample (25 g) at a depth of 16 m. The sample weight is significantly smaller than the traditional weight of ice core samples (0.5 – 1 kg of ice) and the sample weight of the ice core drill chips (~300 g) investigated by Zipf et al. (2016). ^{10}Be-analysis of such small ice samples is possible with the present AMS technology especially from sites where low snow accumulation rates (about 3 cm ice per year) lead to relatively high ^{10}Be concentrations. For example, 50 g-sized ^{10}Be samples from the EPICA Dome C (EDC) ice core were successfully measured at the Tandetron-based AMS facility in Gif-sur-Yvette (France) (Raisbeck et al., 2006). ^{10}Be in even smaller rain water samples (18–51 g) with lower ^{10}Be concentrations, which is matrix-wise similar to molten ice, was also successfully measured at the DREAMS (DREsden Accelerator Mass Spectrometry) facility in Germany (Tiessen et al., 2019).

The major difference in the sample preparation of such small amounts of ice is the possibility to omit ion exchange column (IEC) chemistry. When measuring ^{10}Be in ice or rain water, one has to remove the relatively large volume of melt water, while retaining Be at the same time. This can be achieved by either evaporation or by separation of Be from the melt water using an IEC. Samples as small as 50 g, on the other hand, can fit in most centrifuge tubes (e.g. 50 ml or 100 ml tubes) and, therefore, can be processed without IECs via direct precipitation of $Be(OH)_2$ (Raisbeck et al., 2006). Avoiding the IEC chemistry will save time and resources which is vital for routine measurements of large numbers of ^{10}Be samples. However, some of the deepest ice samples from EDC could not be processed without IECs due to the fact that $Be(OH)_2$ did not precipitate well (Raisbeck et al., 2006). One of the possible reasons given by (Raisbeck et al., 2006) was the interference of drill fluid with the $Be(OH)_2$ precipitation process. Such complications are not expected with the LDC samples since RAID is a dry drilling method, i.e. no drill fluid is used. Nevertheless, it is still important to ensure that ^{10}Be can be extracted from the ice chips without IECs and to test whether the drill chip measurements can be used to assess the atmospheric ^{10}Be production signal similar to measurements on an ice core.

2.1.2. Test samples

Before investigating the small drill chip samples, a suitable and practical method to prepare the ice for AMS measurements needs to be evaluated. A systematic test of the preparation procedure was conducted on various ice samples. The test samples included well-mixed surface ice chips from the LDC site, and snow collected in Lund (Sweden) during the winter of 2018/2019. Due to the high precipitation rate in Lund, the snow samples are expected to have relatively low ^{10}Be concentrations in the same order of magnitude as ice core samples from Greenland. Therefore, the snow was used to test the preparation procedure for possible future ice core projects in Greenland as well as other sites with similar precipitation rates. The test was also conducted on blank samples (i.e., highly purified frozen Milli-Q water).

In a first test, we varied the amount of ^{9}Be carrier for the blank samples, particularly 0.1, 0.15 and 0.2 mg, to evaluate the practical limits for low carrier amounts in the preparation and measurement process. The goal was to determine the optimal amount of ^{9}Be carrier for our AMS measurements in terms of highest measurement efficiency. We define measurement efficiency as the number of $^{9}BeO^{-}$ ions collected in the Faraday Cup on the low energy side of the AMS system within a given measurement time relative to the number of ^{9}Be atoms in the carrier. Secondly, we tested whether the drill chips and small ice samples from high precipitation sites can be processed without IECs. In a standard IEC procedure, Be is extracted from the IEC columns using HCl. Subsequently, $Be(OH)_2$ precipitate will form after raising the pH to the range of 8 - 10 via addition of NH_4OH. However, this process also generates NH_4Cl which could sublimate at ~340°C during the following heating process aiming at oxidising beryllium. This could lead to contamination and/or cause problems to the heating system. Therefore, the $Be(OH)_2$ precipitate is often washed with purified water to remove NH_4^+ and Cl^-. It is noted that the standard ^{9}Be carrier solution could also contain HCl. Since we aim to use a smaller amount of ^{9}Be carrier and to avoid IECs, there is little Cl^- in our samples. Moreover, a step-wise heating process (see details below) will be employed to oxidise $Be(OH)_2$ to BeO which could potentially overcome the sublimation problem. Therefore, we will test whether eliminating the washing step can make the sample preparation procedure more efficient while yielding similarly good results. Finally, our last objective is to test a recently proposed co-precipitation method for Be-cathode preparation that could potentially yield 1.5 times more ion source efficiency at the ETH 6 MV Tandem facility (Christl and Kubik, 2013). This new preparation method involves co-precipitation of

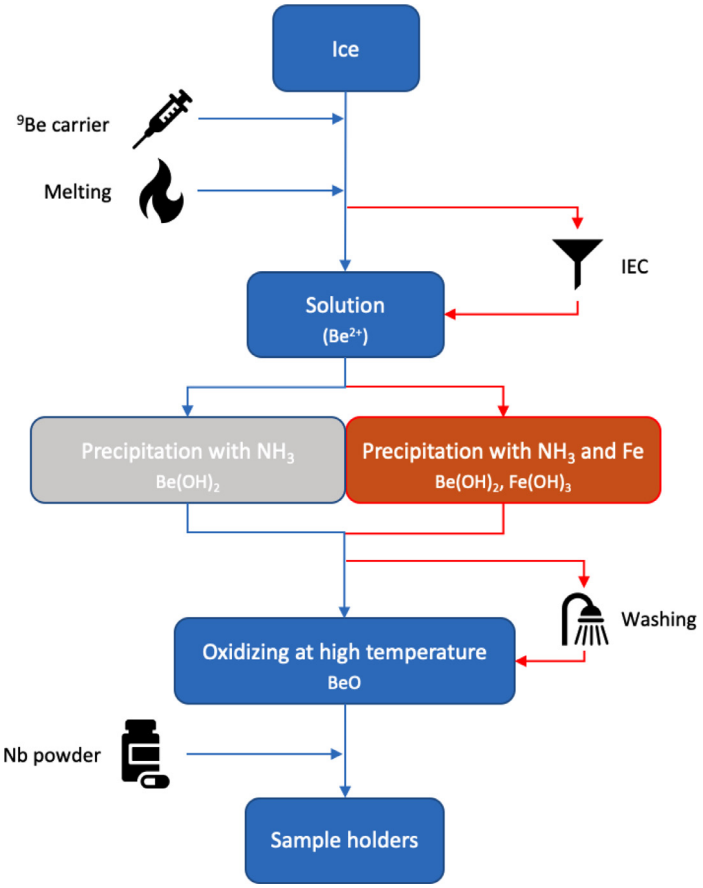

Fig. 1. Summary of the preparation steps for AMS ^{10}Be sample preparation. The steps with the red arrow on the right (IEC, precipitation with Fe and washing) are the processes that we tested in order to determine the most efficient method for the preparation of small ice core samples. (For interpretation of the references to color in this figure legend, the reader is referred to the web version of this article.)

Table 1
Summary of the test sample series.

Sample groups	Procedures	Replicates	+^{9}Be (mg)	+Fe (mg)	Washing	IEC	Nb/Be (at/at)	Fe/Be (at/at)
Blank	*None*	3	0.10	0	No	No	1	0
		3	0.15	0	No	No	0.65	0
		3	0.20	0	No	No	0.5	0
	+	3	0.10	0.15	No	No	1	0.24
	Fe	3	0.15	0.15	No	No	0.65	0.16
		3	0.20	0.15	No	No	0.5	0.12
	Washing+Fe	3	0.10	0.15	Yes	No	1	0.24
		3	0.15	0.15	Yes	No	0.65	0.16
		3	0.20	0.15	Yes	No	0.5	0.12
LDC	*None*	3	0.15	0	No	No	0.65	0
sur-	*+ Fe*	3	0.15	0.15	No	No	0.65	0.16
face	*Washing+Fe*	3	0.15	0.15	Yes	No	0.65	0.16
ice	*IEC+Fe*	3	0.15	0.15	No	Yes	0.65	0.16
~~*Lhipd*~~	*None*	3	0.10	0	No	No	1	0
snow	*+ Fe*	3	0.10	0.15	No	No	1	0.24
	Washing+Fe	3	0.10	0.15	Yes	No	1	0.24
	IEC	3	0.10	0	No	Yes	1	0

$Be(OH)_2$ with Fe before the oxidisation of Be. Subsequently, Nb powder is mixed with BeO (with and without Fe) and pressed into AMS target holders. We will test the samples at the 300 kV MILEA facility of the Laboratory of Ion Beam Physics at ETH Zurich. A better ion source efficiency will significantly increase the measurement quality of samples with low ^{10}Be concentrations.

2.2. Testing the preparation procedure

Fig. 1 summarises the preparation steps (including the testing steps) applied to our ^{10}Be samples. In addition, Table 1 provides the information regarding our test series including sample description, preparation procedures, as well as Nb/Be and Fe/Be mixing ratios. 27 blank samples (50 g of frozen Milli-Q water each) were divided into three groups. For each group, different amounts of ^{9}Be carrier (Scharlau Beryllium 1000 mg/l, $Be_4O(C_2H_3O_2)_6$ in 2% HCl solution) were added to the blanks (0.10, 0.15 and 0.20 mg ^{9}Be per blank) before they were melted in glass beakers. The samples were then transferred into 50 ml plastic centrifugation tubes. 0.15 ml of Fe solution (1000 ppm) was added to two thirds (18/27) of the blank samples before they were precipitated as $Be(OH)_2$ (and Fe-hydroxide) by adding 2 ml of NH_4OH solution (25%) and subsequent centrifugation. The supernatant liquid was discarded from the centrifugation tubes leaving only the gel-like precipitates inside. For half of the blank samples with Fe ($n = 9$), the newly formed precipitates were washed twice with Milli-Q water (pH = 7) to remove NH_4^+ and Cl^-. The

other half ($n = 9$) were not washed. The rest of the samples ($n = 9$) were directly precipitated without adding Fe. All of the blank samples were then transferred into quartz crucibles in order to be oxidised to BeO via a three-step heating process. The heating temperature first stayed at 150 °C for two hours followed by an increase from 150 °C to 850 °C within 2 h, and finally the temperature was held at 850 °C for another two hours. The oxidised blank samples were then mixed with approximately 1 mg of Nb-powder (−325 mesh, 99.8%). The mixtures were pressed into the AMS targets in the final step of the sample preparation.

The surface ice chips were mixed and divided into 12 small samples (50 g each). 0.15 mg carrier was added to the samples before melting as this was considered a preferred carrier amount for these samples. Three of the samples were passed through IECs (Bio-Rad, AG 50W-X8, 100–200 mesh, 0.8 × 4cm). Be^{2+} binding to the IECs was then extracted using 25 ml HCl (4 Mol/L). Be eluted from the IECs was co-precipitated with Fe and NH_4OH solution similar to the blanks. Of the nine samples that were not passed through IECs, six samples were co-precipitated with Fe and NH_4OH and half of latter batch ($n = 3$) was washed twice with Milli-Q water. The three remaining samples were directly precipitated with NH_4OH without adding Fe or washing the precipitate. All of the samples were oxidised (same heating steps as the blanks) before mixing with approximately 1 mg Nb-powder and pressing into the sample holders.

The snow sample from Lund was also mixed and divided into 12 smaller samples (50 g each) which were then prepared with the same protocol as the surface ice chips. However, the samples that had passed through IECs were directly precipitated without additional Fe. In addition, only 0.1 mg carrier was added to all of the snow samples. A smaller amount of ^{9}Be carrier was used here because of the relatively low ^{10}Be content of the snow which could otherwise result in too low ^{10}Be/^{9}Be ratios. Lower ^{10}Be/^{9}Be ratios will lead to larger measurement errors due to the background correction uncertainties.

Overall, three replicates were produced for each test group and the results can be used for statistical analysis. In total, five different preparation procedures were tested including “None”, “+ Fe”, “Washing + Fe”, “IEC + Fe” and “IEC” (see Table 1). In addition, different amounts of ^{9}Be carrier were tested for the blank samples, i.e. 0.10 mg, 0.15 mg and 0.20 mg (Table 1). All of the measurements were performed at the ETH Zurich 300 kV MILEA AMS facility. The measurement time for all samples was between 20 and 25 min, except for one surface ice chip sample that had a counting time of 12 min (figure S3).

For each group, we performed an analysis of variance (ANOVA) (Ståhle and Wold, 1989) to investigate the effects of the procedures listed in Table 1 on the measured ^{10}Be/^{9}Be ratio, the BeO ion current and the relative measurement error. We also analysed whether the amount of ^{9}Be carrier had an impact on our results for the blank samples. For instance, we computed the variance in the results depending on the different procedures and/or the ^{9}Be carrier amount. This explainable variance was then divided by the residual (unexplainable) variance in the results to derive the so-called F-statistic. A F-statistic significantly larger than 1.0 means that most of the variance can be predicted by independent variables (i.e. the different procedures and/or the amount of ^{9}Be carrier) and therefore indicates the effects of the independent variables on the results (Ståhle and Wold, 1989). A F-test was then conducted assuming the F-statistic following an F-distribution under the null hypothesis that the different procedures and the amount of carrier do not have any influence on the performance parameters and on the ^{10}Be/^{9}Be ratio (i.e. the probability of obtaining a large F-statistic is low). The significance of the F-statistic is indicated by the p-value that is the probability of obtaining a larger value than the F-statistic. The larger the F-statistic the smaller is the p-value. The effects of the independent variables are commonly considered significant if the p-value is smaller than 0.05.

3. Results and discussion

3.1. Test sample results

Fig. 2 displays the results of ^{10}Be/^{9}Be measurements. The black symbols in the figure illustrate the samples that were prepared with the simplest procedure, i.e. no IEC, no washing of the $Be(OH)_2$ precipitate and no addition of Fe (“None” in Table 1). The test samples with additional Fe (“+Fe” in Table 1) are indicated in orange and the test samples that were washed and co-precipitate with Fe (“Wash + Fe” in Table 1) are shown in blue. Finally the test samples processed with IECs (“IEC” and “IEC + Fe” in Table 1) are shown in green.

The isotopic ratios of the blank samples (Fig. 2a) spanned from 0.3×10^{-14} to 1.6×10^{-14}. Our ANOVA results (table S1, supplementary) show a significant decrease in the ^{10}Be/^{9}Be ratio with increasing ^{9}Be amount for the samples that followed the “None” procedure (p-value = 0.02*) and the samples with Fe (p-value = 0.03*). The decreasing ratios with increasing ^{9}Be carrier amount (black and orange squares in Fig. 2a) could indicate a constant contamination with ^{10}Be (independent of the carrier) during the sample preparation. However, no significantly decreasing trend was found (p-value = 0.15) for the washed samples (blue squares in Fig. 2). On the contrary, an increase in the carrier amount from 0.15 mg to 0.20 mg corresponds to a rise in the ^{10}Be/^{9}Be ratio of washed samples from 0.9×10^{-14} ($\pm 0.16 \times 10^{-14}$) to 1.4×10^{-14} ($\pm 0.16 \times 10^{-14}$). One possible explanation for this unexpected result is that the washing step increased the ^{10}Be contamination due to dust input and possibly (but rather unlikely) some ^{10}Be in the Milli-Q water used for the washing step. However, the exact cause of this slight elevation in ^{10}Be/^{9}Be ratio is uncertain and the statistical basis for this observation is weak. Also, at such low levels even alternative explanations such as ^{10}Be in the Nb powder or in the target holders cannot be excluded.

Fig. 2b and c show that different preparation procedures i.e., adding Fe, IEC chemistry and washing Be-hydroxide did not significantly influence the ^{10}Be/^{9}Be ratios ($p = 0.41$ and 0.39, respectively, table S2). Hence, all of the procedures have led to comparable results. However, the washed samples of surface ice chips and Lund snow (blue colour) had somewhat inconsistent results among the replicates. We conducted a chi-squared test (Montgomery and Runger, 2018) to investigate the effect of the different procedures on the ^{10}Be concentrations (at/g) among the replicates (figure S1, supplementary). The results indicate that the washed blank samples with 0.1 mg ^{9}Be carrier, and the washed samples from surface ice chips and Lund snow showed significant differences among the replicates. The χ^2 test statistics of these washed samples were 6.4, 8.9 and 10.6, respectively, exceeding the 95% confidence interval of a one-sided chi-square test (around 6 with two degrees of freedom). This inconsistency illustrates that the washing step has led to less reproducible results in our tests. The previously proposed hypothesis that the washing step increases possible contamination risk is consistent with this observation even though, to our knowledge, there is no obvious process that could lead to a contamination during the washing process.

Fig. 3 shows the development of the BeO-current during the AMS measurement for the blank samples. The current is shown as average BeO-current per pass, with one pass lasting 112 s. According to expectations, a higher ^{9}Be carrier amount generally resulted in a higher current. Blank samples containing Fe (Fig. 3b and c) have led to more reproducible currents with better agreement between the three replicates. Moreover, “+ Fe” samples (Fig. 3b) did not show a decreasing trend even after 25 min measurement time. Thus, they could potentially be measured for a longer time which would allow for a reduction of the measurement uncertainty. Meanwhile, the “None” samples (Fig. 3a) had BeO-currents that peaked around 10 to 15 min and mostly decreased afterward. These results also show that the total efficiency (Fig. 4b) can be significantly increased by longer measurement times. Similar results are observed for the samples of surface ice chips and Lund snow (Fig. S2 and S3, supplementary information).

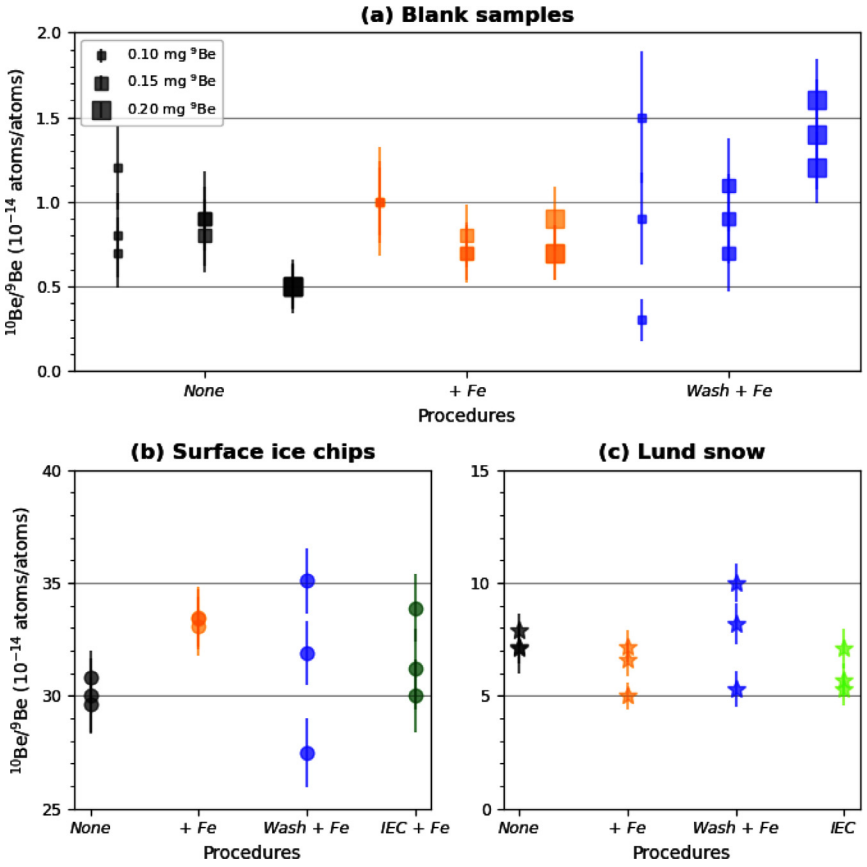

Fig. 2. The ^{10}Be/^{9}Be isotopic ratio (± 1-σ measurement uncertainties) of the blank samples (a), and of the LDC surface ice chips (b) and Lund snow (c). Different procedures are indicated by different colours. The amount of ^{9}Be carrier in the blank samples is represented by the size of the symbols (small size for 0.1 mg, medium size for 0.15 mg and large size for 0.2 mg ^{9}Be carrier). The ^{10}Be/^{9}Be ratios of blank samples tend to decrease with increasing ^{9}Be amount, except for the blank samples prepared with the "Wash + Fe" procedure (blue symbols, panel a). The amount of ^{9}Be carrier used to prepare the ice chips and snow was 0.15 mg and 0.10 mg, respectively. Different preparation methods mostly produced similar ^{10}Be/^{9}Be results that agree within measurement uncertainties. (For interpretation of the references to color in this figure legend, the reader is referred to the web version of this article.)

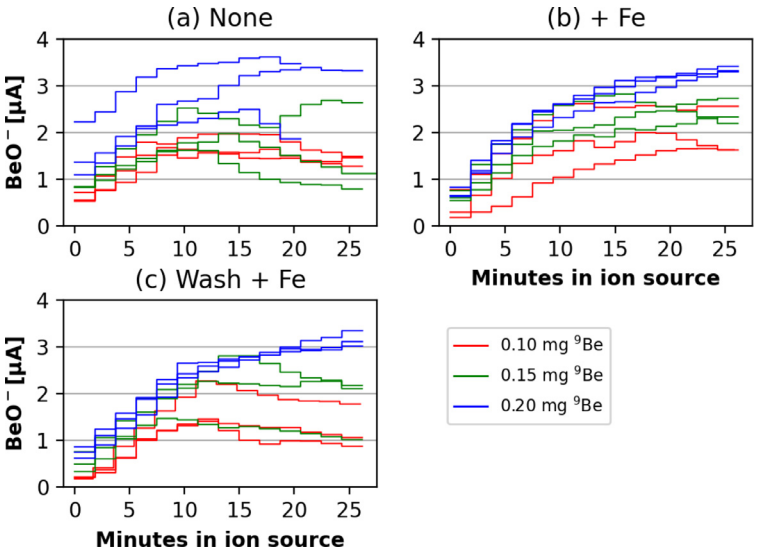

Fig. 3. AMS BeO-current development for different preparation procedures of the blank samples, i.e. (a) "None", (b) "+ Fe", and (c) "Wash + Fe". The different amount of ^{9}Be carrier is represented by the different colours. Blank samples containing Fe (subplots b and c) had a more similar BeO-current development among the three replicates. Also, the current of "+ Fe" samples (b) did not decrease even after 25 min measurement time. Therefore, adding Fe could potentially lead to more reproducible results and smaller measurement uncertainties via a longer measurement time. (For interpretation of the references to color in this figure legend, the reader is referred to the web version of this article.)

The average BeO-currents are shown in Fig. 4a. The averages represent the 25-min measurement time for blank samples and the 20-min measurement time for the other samples (LDC surface ice chips and Lund snow). As expected, the amount of ^{9}Be significantly affected the average AMS ion current of the blank samples (p-value < 0.01*, table S1). The average BeO-currents of the blank samples increased by about 0.6 μA for a 0.05 mg ^{9}Be carrier increment. On the other hand, the amount of ^{9}Be carrier should not be too large to ensure that the ^{10}Be/^{9}Be ratio of ice samples remains considerably higher than that of the blank samples. Ideally, the ^{10}Be/^{9}Be ratio of blank samples should be below 5–10% of the ^{10}Be/^{9}Be ratio of the small ice samples. In this case, a blank correction (i.e. the subtraction of the blank ratio from the sample ratio) will not increase the measurement uncertainties significantly. If we consider the "None" procedure, for example, the Lund samples and the LDC samples contained on average 1.0×10^4 and 6.0×10^4 ^{10}Be atoms per gram, respectively. They produced ^{10}Be/^{9}Be ratios of 7.4×10^{-14} (snow) and 30.1×10^{-14} (surface ice chips) on average, with 0.10 mg and 0.15 mg ^{9}Be carrier, respectively (Fig. 2c and b). These ratios are significantly higher than the corresponding blank ratios which were 0.90×10^{-14} and 0.87×10^{-14} on average for 0.10 mg and 0.15 mg ^{9}Be carrier, respectively. Therefore, the blank correction will give good results in the tested cases. In summary, there is always a trade-off between ^{10}Be/^{9}Be

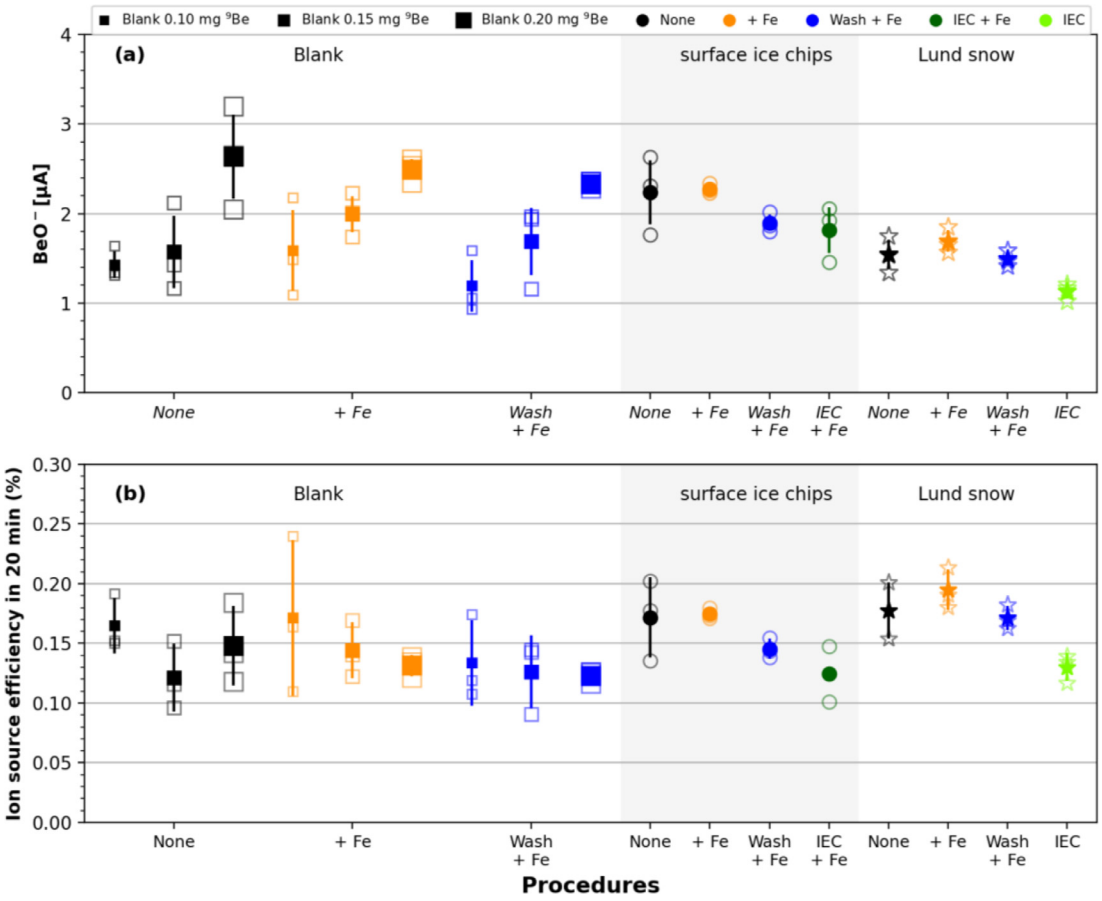

Fig. 4. The average measurement current (a) and apparent measurement efficiency for ^{9}Be (BeO) based on 20 min measurement time (b). Different procedures and sample groups are represented by different colours and symbols. One "IEC + Fe" sample from LDC was excluded (in panel b) due to significantly shorter measurement time. Different preparation procedures mostly resulted in similar average measurement current and apparent measurement efficiency, except for the samples processed with IECs (green colour) which tended to reduce the average current as well as the efficiency. (For interpretation of the references to color in this figure legend, the reader is referred to the web version of this article.)

ratios well above the background level versus good currents that lead to sufficiently long measurement times.

Fig. 4a shows that different preparation procedures did not significantly influence the average measurement current of the surface ice chip samples (p-value=0.17, table S2). The "IEC + Fe" and the "Wash + Fe" samples of the surface ice chips had lower current, on average, than the "None" samples and the "+ Fe" samples (Fig. 4a). However, this reduction in current was not statistically significant. On the other hand, we found a significant effect of the different procedures on the average BeO current for the snow samples (p-value < 0.01*, table S2). Here, the average current of the "IEC" samples was about 0.56 μA lower than for the other samples (Fig. 4a) indicating that Be was potentially lost during the IEC process of the Lund samples. A possible reason is an incomplete extraction/recovery of Be^{2+} from the IECs. This results in a correct ^{10}Be/^{9}Be (as seen in Fig. 2c) but a lower measurement current which can affect the required measurement time and the final uncertainty.

We assessed the apparent ionisation efficiency of the ion source (Fig. 4b) by integrating the negative BeO ion current over 20 min and by dividing this value by the total number of Be atoms in the sample. The more BeO ions can enter the AMS system within a given measurement time the better the combined performance of the preparation method and the AMS system (Christl and Kubik, 2013). Fig. 4b also shows that different preparation procedures do not significantly influence the ion source efficiency except for the "IEC + Fe" procedure of Lund snow, which resulted in an average efficiency lower than the other procedures by 0.05%. This result is mirrored by the average current out of the ion source (Fig. 4a) as discussed above. On the other hand, adding Fe did not result in an increased ion source efficiency within the default measurement time.

In conclusion, our test samples could be prepared without the use of IECs. The $Be(OH)_2$ precipitated well and the resulting ^{10}Be/^{9}Be ratios showed no problem. Washing the $Be(OH)_2$ precipitate was also not necessary for the test samples. Although co-precipitation of the samples with Fe did not result in an increased ion source efficiency, the procedure generated more reproducible measurement currents and also offers the opportunity for higher efficiencies via longer measurement times. In addition, adding Fe helped handling the sample better throughout the preparation process due to the better visibility of the Be hydroxide/iron precipitate. The co-precipitation of Be with Fe produced a reddish-brown colour from $Fe(OH)_3$ instead of a white translucent colour from $Be(OH)_2$ only. This allows for a better identification and handling of the samples and therefore reduces the probability of losing sample material. This can lead to more precise measurement results, especially when many samples are prepared on a routine basis.

3.2. Achievable measurement uncertainties

Fig. 5 illustrates the dependence of the relative measurement uncertainty on the total number of ^{10}Be atoms in the samples and the efficiency in detecting those ^{10}Be atoms within a given measurement time. The total apparent efficiency (i.e. the number of ^{10}Be atoms detected by AMS within a given measurement time divided by total number of ^{10}Be atoms in the sample) could significantly influence the results for

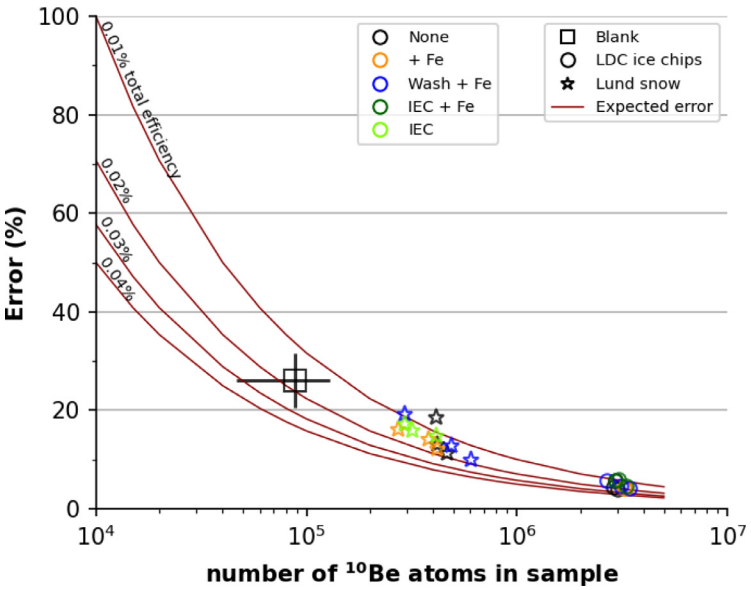

Fig. 5. The measurement uncertainty as function of the number of ^{10}Be atoms per sample and total efficiency for a given measurement time of 25 min (blanks) and 20 min (other samples). The mean and ± 1-σ error of the blank samples are represented by the big black square. For the ice chips and snow, the results after background correction (see text for details) of different sample groups and procedures are indicated by different symbols and colours. The red lines represent the expected relative error (assuming that the counting statistics is dominating the final uncertainty) according to different levels of total efficiency. Most of our test samples were measured at a total efficiency of about 0.01% - 0.02%. In addition, the measurement uncertainties were mainly determined by the number of ^{10}Be atoms in the samples. (For interpretation of the references to color in this figure legend, the reader is referred to the web version of this article.)

samples with a low amount of ^{10}Be, e.g. the snow samples and comparable samples from Greenland of the same size. The influence on relative measurement error was not an issue for samples with relatively high concentrations of ^{10}Be atoms such as the LDC ice chips. Most of our test samples had a total apparent efficiency of about 0.01% to 0.02% which means that within the given measurement time (20–25 min/sample) about one or two ^{10}Be atoms can be detected for every 10,000 ^{10}Be atoms in the sample. The measurement time could have been prolonged for all samples (see Fig. 3 and also Fig. S2 and S3) which would further increase the number of ^{10}Be detections per sample and therefore the total apparent efficiency.

The number of ^{10}Be atoms measured in the 50 g blank samples ($8.8 \times 10^4 \pm 4.1 \times 10^4$ atoms, black squares in Fig. 5) indicated the background levels for 50 ml MilliQ "samples". We did a background correction for the samples of LDC surface ice chips and Lund snow. We subtracted the blank ^{10}Be/^{9}Be ratio, and incorporated the measurement uncertainties of the blank samples to the measurement uncertainties of the ice and snow samples. As shown above, different preparation methods have led to similar ^{10}Be/^{9}Be results. Therefore, we used the average results of all blank samples with 0.15 mg ^{9}Be carrier to correct for the LDC samples, and the average results of all blank samples with 0.10 mg ^{9}Be carrier to correct for the Lund snow samples. The stars in Fig. 5 symbolise the snow samples from Lund that contained on average 39.8×10^4 ($\pm 9.2 \times 10^4$) ^{10}Be atoms and had a mean measurement uncertainty of 14.6% (± 2.8%). The 50 g LDC surface ice chips (circle symbols in Fig. 5) contained on average 309.5×10^4 ($\pm 21.2 \times 10^4$) ^{10}Be atoms, which is six times higher than in the snow from Lund. The measurement uncertainty of the surface ice chips (4.8% ± 0.7%) was consequently lower than for the snow samples. On the other hand, we found no significant effect of the different procedures on the relative error of the surface ice chip and Lund snow measurements (p-value = 0.25 and 0.85, respectively, table S2).

3.3. Quality and potential of a novel ^{10}Be record from the LDC deep ice chips retrieved with RAID

In the following we show results where we applied the "+Fe" preparation procedure with 0.15 mg ^{9}Be carrier to prepare the LDC deep ice chips retrieved with RAID. Each of the samples covered a depth ranging from 21.5 cm to 66.7 cm with a mean depth resolution of 43.6 cm. Our deep ice chips from LDC are from a location close to the drill site of the EDC ice core (75°05′59″S, 123°20′59″E). Therefore, we can as a first-order estimation transfer the EDC time scale to our LDC samples. The sampling resolution (i.e. number of years represented by each ice chip sample) is expected to vary between 4 and 15 years (depending on depth range, compaction and depth) according to the chronology of the EDC ice core (figure S4) (Parrenin et al., 2007).

We also prepared and measured a blank sample for every 10 or 15 samples of ice chips to keep track of the background ^{10}Be concentration. The blank correction was conducted by subtracting the background ^{10}Be/^{9}Be ratio indicated by the blank samples from the ^{10}Be/^{9}Be ratio of the ice chip samples, and incorporating the measurement uncertainty of the blank samples to the measurement uncertainty of the corresponding ice chips samples via error propagation. The result of ^{10}Be concentrations and associated measurement uncertainties (after blank correction) are shown in Fig. 6. ^{10}Be concentrations of the LDC deep ice chips range from around 3.8×10^4 to 8.0×10^4 at/g with a mean of 5.7×10^4 at/g. AMS measurement uncertainties range from about 2.2% to 5.5% with a mean of 3.3%. The sample with the smallest weight of 25 g has a measurement uncertainty of 4.3%. The sample on top, which is closest to the surface, is likely to have an age spanning from 2013 to 2017 C.E. according to the EDC chronology. This top sample has a ^{10}Be concentration of 5.5×10^4 ($\pm 0.2 \times 10^4$) at/g lower than the ^{10}Be concentration in 2017 C.E. which is 6.2×10^4 ($\pm 0.3 \times 10^4$) at/g recorded in the surface ice chips. The reason might be that solar activity was stronger between 2013 and 2016 C.E. (Svalgaard and Schatten, 2016) and consequently less ^{10}Be was produced in the atmosphere.

Fig. 7a shows the comparison to ^{10}Be concentrations from the South Pole ice core (Raisbeck et al., 1990) and the global ^{14}C production rate. Periods of extended low solar activity can be observed as periods of enhanced ^{10}Be concentrations. For example, the Spörer Minimum from around 1450 to 1550 C.E. and the Maunder Minimum from around 1645 to 1715 C.E. are observed around 25–30 and 18–23 m depth, respectively. The solar minima visible in the LDC ^{10}Be concentrations were synchronised (Fig. 7a) to the mean global ^{14}C production rate inferred from IntCal20 (Reimer et al., 2020) via carbon cycle modelling (Reimer et al., 2020; Siegenthaler, 1983). The uncertainties in the new IntCal20 calibration curve were included by using 100 posterior realisations of possible atmospheric ^{14}C curves obtained by fitting Bayesian splines to the ^{14}C data underlying IntCal20 (Reimer et al., 2020; Heaton et al., 2020). Here we report the average ^{14}C production rate obtained from the 100 calculations. The surge in atmospheric CO_2 from 1850 C.E. due to fossil-fuel burning was also included to account for the dilution of ^{14}C in relation to ^{12}C (Muscheler et al., 2007). The

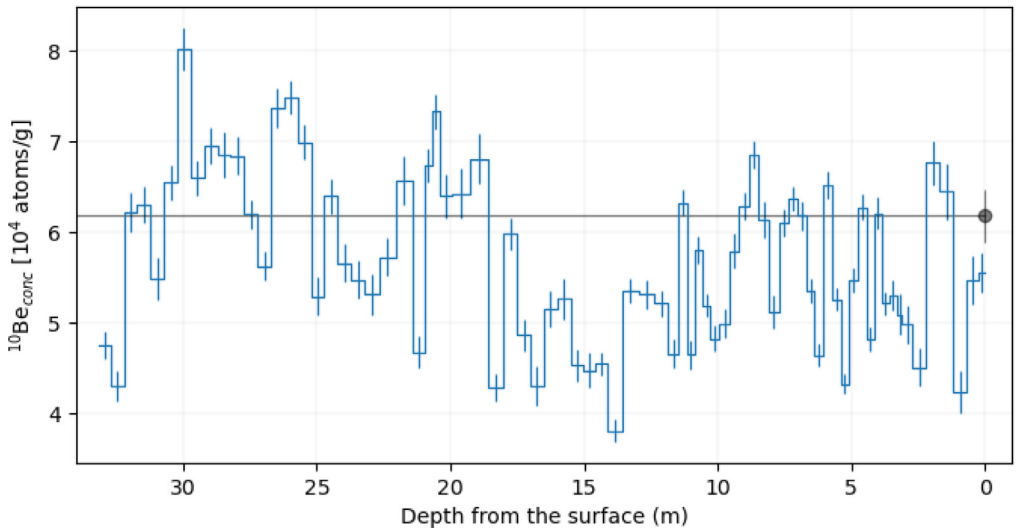

Fig. 6. ^{10}Be concentrations and associated measurement uncertainties of the LDC ice chips drilled with RAID. The black dot and black line show the mean ^{10}Be concentration and average measurement uncertainty of the tested surface ice chips (after blank correction) for comparison.

^{14}C production rate was normalised to the pre-industrial mean. The two records of ^{10}Be and ^{14}C are expected to show the same relative changes as a result of the varying production rates through solar and geomagnetic shielding (Muscheler et al., 2007). This allows us to refine the timescale of RAID samples via the established ^{14}C timescale.

The timescale presented here (Fig. 7a) is a preliminary timescale of the LDC samples. The uncertainties of ice core timescales obtained via this ^{10}Be to ^{14}C synchronisation method around the investigated time interval are typically in the ranges of 5–10 years (Adolphi and Muscheler, 2016). The synchronisation uncertainties also rely on temporal resolution of the data and therefore will be different for different sections. The LDC timescale agrees well with the EDC time scale above the depth of 24 m (figure S4). Below that depth, the estimated LDC timescale shows an older age than the EDC timescale at the same depth. The age difference increases gradually to 40 years at the depth of 32 m.

The ^{10}Be concentrations measured in the ice chips agree relatively well with the mean ^{14}C production rate (r= 0.58, Fig. 7a) and the ^{10}Be concentrations from the South Pole ice core (r= 0.47, Fig. 7a), especially around the Spörer Minimum and the Maunder Minimum. However, the LDC samples show larger variability after 1850 C.E. compared to the other records. This difference potentially originates from the transport and deposition processes of the radionuclides. For example, ^{10}Be concentrations in ice cores are likely affected by the local weather and climate conditions during the atmospheric transport and deposition process of ^{10}Be (Muscheler et al., 2016; Field et al., 2006; Heikkilä and Smith, 2013; Pedro et al., 2006; Pedro et al., 2011; Pedro et al., 2012; Zheng et al., 2020) and potentially also by stratospheric volcanic eruptions (Baroni et al., 2019). The larger variations could be induced by the relatively high sampling resolution in the top layers of the LDC ice chips (4–8 years per samples) and potentially some randomness in the sampling of the rather soft top layers. In comparison, the sampling resolution of the top layers of the South Pole ice core was 6–14 years per sample (Raisbeck et al., 1990) which resulted in more smoothening and therefore less variability. In addition, the measured ^{14}C records are influenced by the global carbon cycle mainly through fossil fuel burning, that, however, has been included in the calculation of the ^{14}C production rate (Muscheler et al., 2007). Nevertheless, it is possible that the carbon cycle effects could not be eliminated completely by our box-diffusion model and that the smoothed IntCal20 data set does not capture the full range of ^{14}C variability. These reasons could explain the differences in short-term variations between the records.

The short-term weather and climate signals and the poorly resolved 11-year solar cycle can be removed via computing 25-year running averages of the normalised ^{10}Be concentrations (Vonmoos et al., 2006). The remaining long-term changes in the ^{10}Be concentrations of the ice chips agreed better with the running mean of ^{14}C production rate (r= 0.72, Fig. 7b) and the running mean of the ^{10}Be concentrations from the South Pole ice core (r= 0.74, Fig. 7b). This shows that the ice chips drilled with RAID are promising samples for assessing the long-term changes in the ^{10}Be deposition rate at different ice core sites with benefits for improving the assessment of long-term solar and geomagnetic shielding of galactic cosmic rays.

There was potential smoothing in the ^{10}Be concentrations because of possible mixing of drill chips in the barrel during each run while drilling the ice chips. Even though the sampling procedure was done in order to get a good average sample for each depth interval, there is still the possibility of some randomness in the sampling procedure. Possible mixing was tested using a realisation of the ^{14}C production rate (randomly selected among the 100 realisations), since the mean production rate of ^{14}C was too smooth compared to the ^{10}Be data. The annual ^{14}C production rate of the selected realisation was averaged to achieve the same temporal resolution as the ^{10}Be data (blue line in Fig. 8). We then assumed an increase in the depth range for each ice sample by 10 cm (5 cm on each side) to simulate a 10-cm mixing scenario and computed new ages for the temporal coverage of the ^{10}Be samples. Subsequently, we re-averaged the ^{14}C production rate with the new temporal resolution (orange line in Fig. 8). This assumed mixing scenario leads to a decreased temporal resolution of 3.3 to 4.9 years compared to the unmixed scenario. There was significant reduction in variation of the ^{14}C production rate, especially after 1830 C.E. where the samples cover the shortest time intervals. Several adjacent samples substantially overlap in this scenario and, therefore, show very similar values for the ^{14}C production rate. On the other hand, the LDC ^{10}Be concentrations after 1800 C.E. show significant short-term variability indicating that the ice samples were unlikely to be well mixed. Furthermore, from the drilling and sampling procedure we expect that the 10 cm mixing scenario is rather a worst-case assumption. In conclusion all these considerations suggest a level of smoothing that is negligible for medium to long-term studies of ^{10}Be deposition.

4. Conclusion

We conducted a systematic test of different ice sample preparation procedures for ^{10}Be AMS measurement to determine a suitable and prac-

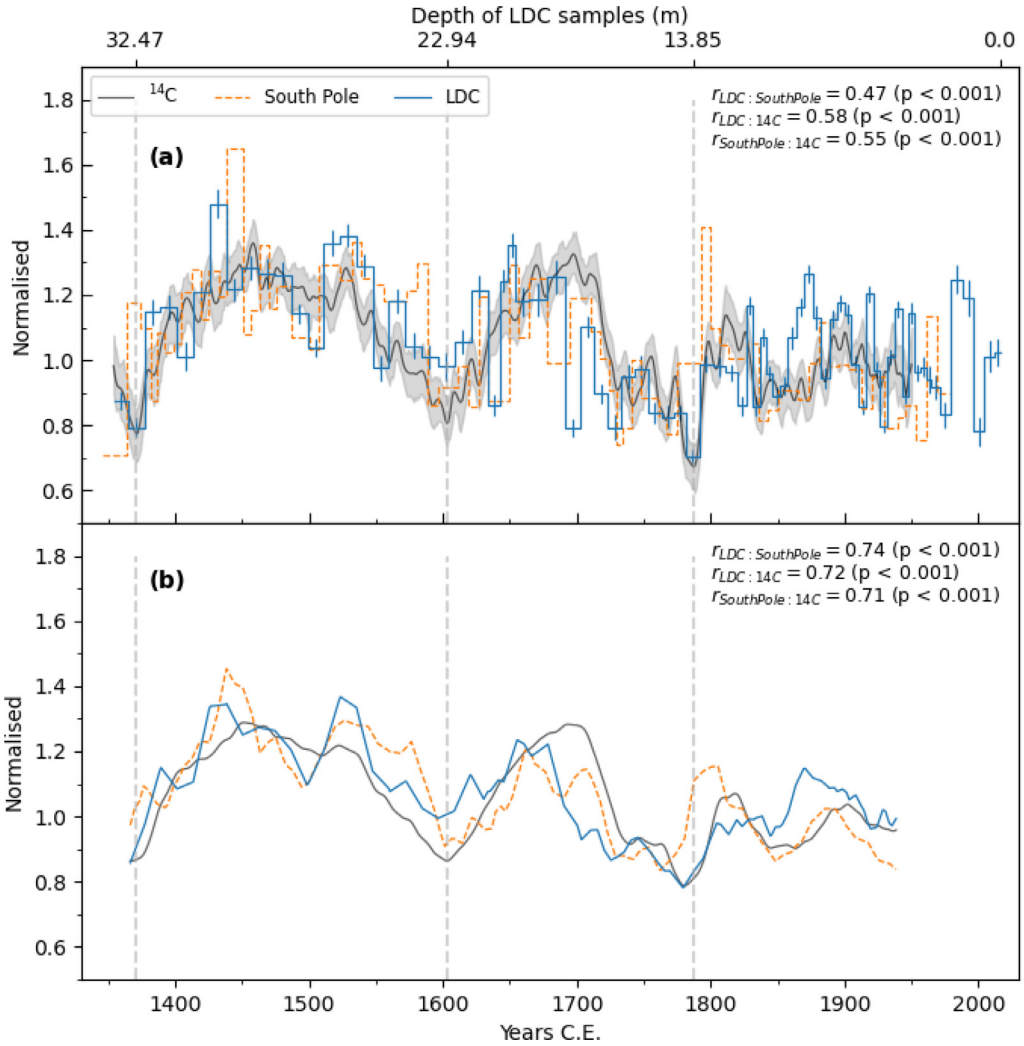

Fig. 7. (a) Normalised ^{10}Be concentrations from the LDC drill chips (solid blue line) and the South Pole ice core (Raisbeck et al., 1990) (dashed orange line) in comparison to the normalised mean ^{14}C production rate (black solid line). The ^{14}C production rate was normalised to the pre-industrial mean, and the ^{10}Be concentrations was normalised to have the same mean with the ^{14}C production rate for the period of overlap. The grey band depicts the 95% confidence interval of 100 ^{14}C production rate realisations. The ^{14}C production rate is shown at annual resolution but is smoothed due to the construction of the average IntCal20 ^{14}C record (Reimer et al., 2020). The vertical grey lines demonstrate synchronisation points for ^{10}Be concentration from LDC ice chips to the ^{14}C production rate. Panel (b) shows 25-year running means of the ^{14}C production rate and ^{10}Be concentrations for the period from 1354 to 1950 C.E.. The correlation coefficients and associated significance levels are also shown. The long-term changes in ^{10}Be concentration of the LDC ice chips agree well with the long-term variations in the ^{10}Be concentration from the South Pole ice core and in the ^{14}C production rate. (For interpretation of the references to color in this figure legend, the reader is referred to the web version of this article.)

tical method to prepare small ice-core ^{10}Be samples such as the LDC ice chips. Our results show that a relatively small amount of ^{9}Be carrier can be used to achieve a good balance between ^{10}Be/^{9}Be ratio and BeO negative ion current at the AMS facility at the Ion Beam Physics laboratory at ETH Zurich. In particular, we used 0.15 mg ^{9}Be carrier for the LDC ice chips and 0.1 mg ^{9}Be carrier for samples with lower ^{10}Be concentrations. In addition, our small ice samples (~50 g of ice) did not need to be processed with IECs or washed with purified water after precipitation of $Be(OH)_2$. Meanwhile, co-precipitation of the samples with Fe offers the opportunity for higher efficiencies via longer measurement times and better handling of the ice samples due to the hue of the Be hydroxide/iron precipitate. Our simplified preparation procedure could be applied not only for the LDC ice chips but also for small ice samples from high precipitation sites such as Greenland and West Antarctica.

The small samples of LDC ice chips (25–45 g) retrieved with RAID were prepared with the simplified preparation procedure. The resulting ^{10}Be concentrations clearly show various solar minima, i.e. the Spörer Minimum from around 1450 to 1550 C.E. and the Maunder Minimum from around 1645 to 1715 C.E.. The initial timescale of LDC ice chips could be improved via synchronisation of the solar minima to the timescale of the global ^{14}C production rate. The longer-term variations of ^{10}Be concentrations measured in the LDC ice chips agreed well with the ^{10}Be concentrations in the South Pole ice core and the ^{14}C production rate and, thus, reflect well the atmospheric production signal. On the other hand, we also assessed the potential of mixing among the ice chip samples during the process of drilling and retrieving the ice. Our assessment shows that the mixing could decrease the targeted temporal resolution. However, for our sample depth from 0 to 33.5 m (corresponding to the time period from 2017 back to 1354 C.E.) the temporal resolution likely decreases less than 3 to 5 years due to drill chips mixing. This can be considered insignificant for medium to long-term ^{10}Be studies. Therefore, we conclude that ice chips retrieved with RAID are promising samples for assessing the long-term changes in ^{10}Be deposition at different ice core sites. These novel ^{10}Be ice chip samples are recovered faster than the traditional ice-core samples and small ice chip samples ($\leq$ 50 g) can be relatively quickly prepared for AMS measure-

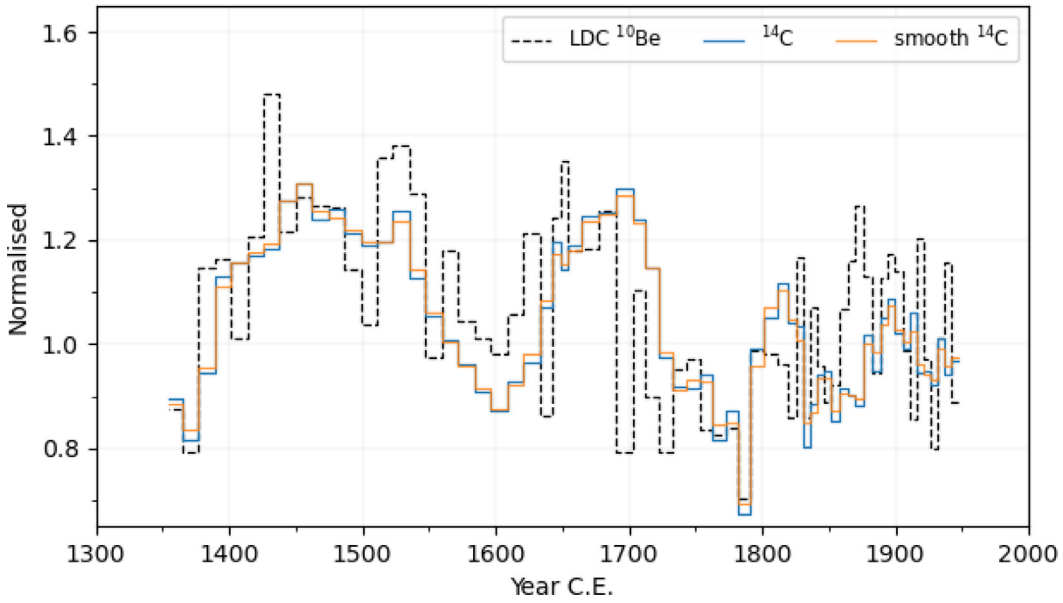

Fig. 8. Possible effects of a drill-chip mixing scenario (see text) illustrated via its corresponding smoothing effect on the ^{14}C global production rate. The black dashed lines show the ^{10}Be concentrations in the LDC ice chips. The blue line shows the binned (averaged) version of the annual ^{14}C production rate with the same temporal resolution as the ^{10}Be data. The orange line shows the effects of a smoothing scenario with a 10 cm depth mixing of the drill chips. The comparison shows that a 10 cm mixing scenario can be considered an upper limit for the mixing of drill chips. (For interpretation of the references to color in this figure legend, the reader is referred to the web version of this article.)

ments. This creates an opportunity for fast recovery of ice samples for continuous ^{10}Be records that depend less on major ice-core projects. This could help us to improve the assessment of long-term solar and geomagnetic shielding of galactic cosmic rays.

Declaration of Competing Interest

The authors declare that they have no known competing financial interests or personal relationships that could have appeared to influence the work reported in this paper.

Acknowledgements

This publication was generated in the frame of Beyond EPICA. The project has received funding from the European Union's Horizon 2020 research and innovation programme under grant agreement No. 815384 (Oldest Ice Core). It is supported by national partners and funding agencies in Belgium, Denmark, France, Germany, Italy, Norway, Sweden, Switzerland, The Netherlands and the United Kingdom. We acknowledge the generous support of the Crafoord foundation for the Swedish national contribution to Beyond EPICA. Logistic support is mainly provided by ENEA and IPEV through the Concordia Station system. This publication also benefitted from support by the Swedish Research Council Grant (grant number DNR2013-8421 and DNR2018-05469 to Raimund Muscheler) and the Royal Physiographic Society of Lund. The opinions expressed and arguments employed herein do not necessarily reflect the official views of the European Union funding agency or other national funding bodies. This is Beyond EPICA publication number 23.

Supplementary materials

Supplementary material associated with this article can be found, in the online version, at doi:10.1016/j.ringeo.2021.100012.

Reference

Adolphi, F., & Muscheler, R. (2016). Synchronizing the Greenland ice core and radiocarbon timescales over the Holocene – Bayesian wiggle-matching of cosmogenic radionuclide records. *Climate of the Past, 12*, 15–30 https://doi.org/. 10.5194/cp-12-15-2016.

Alley, R. B. (1995). Changes in continental and sea-salt atmospheric loadings in central Greenland during the most recent deglaciation: model-based estimates. *Journal of Glaciology, 41*, 503–514 https://doi.org/. 10.1017/S0022143000034845.

Baroni, M., Bard, E., Petit, J. R., & Viseur, S. (2019). Persistent draining of the stratospheric 10Be reservoir after the Samalas Volcanic Eruption (1257 CE). *Journal of Geophysical Research, [Atmospheres], 124*, 7082–7097 https://doi.org/. 10.1029/2018JD029823.

Christl, M., & Kubik, P. W. (2013). New Be-cathode preparation method for the ETH 6 MV Tandem. In *Nucl. Instruments Methods Phys. Res. Sect. B Beam Interact. with Mater. Atoms* (pp. 199–202). North-Holland. https://doi.org/. 10.1016/j.nimb.2012.03.031.

Christl, M., Maden, C., Kubik, P. W., Müller, A., Ivy-Ochs, S., & Suter, M. (2010). Carrier-free measurements of natural 10Be/9Be ratios at low energies. In *Nucl. Instruments Methods Phys. Res. Sect. B Beam Interact. with Mater. Atoms.: 268* (pp. 726–729). https://doi.org/. 10.1016/J.NIMB.2009.10.015.

F. ield, C. V., Schmidt, G. A., Koch, D., & Salyk, C. (2006). Modeling production and climate-related impacts on 10Be concentration in ice cores. *Journal of Geophysical Research, [Atmospheres]*, 111 https://doi.org/. 10.1029/2005JD006410.

Heaton, T. J., Blaauw, M., Blackwell, P. G., Bronk Ramsey, C., Reimer, P. J., & Scott, E. M. (2020). The IntCal20 approach to radiocarbon calibration curve construction: a new methodology using Bayesian splines and errors-in-variables. *Radiocarbon, 62*, 821–863 https://doi.org/. 10.1017/RDC.2020.46.

Heikkilä, U., & Smith, A. M. (2013). Production rate and climate influences on the variability of 10Be deposition simulated by ECHAM5-HAM: Globally, in Greenland, and in Antarctica. *Journal of Geophysical Research, [Atmospheres], 118*, 2506–2520 https://doi.org/. 10.1002/jgrd.50217.

Korschinek, G., Bergmaier, A., Faestermann, T., Gerstmann, U. C., Knie, K., & Rugel, G. (2010). A new value for the half-life of 10Be by heavy-ion elastic recoil detection and liquid scintillation counting. *Nuclear Instruments and Methods in Physics Research Section B: Beam Interactions with Materials and Atoms., 268*, 187–191 https://doi.org/. 10.1016/j.nimb.2009.09.020.

Kutschera, W. (2013). Applications of accelerator mass spectrometry. *International Journal of Mass Spectrometry, 349–350*, 203–218 https://doi.org/. 10.1016/j.ijms.2013.05.023.

Lachner, J., Ploner, M., Steier, P., Sakaguchi, A., & Usui, A. (2020). Accumulation of ferromanganese crusts derived from carrier-free 10Be/9Be. *Nuclear Instruments and Methods in Physics Research Section B: Beam Interactions with Materials and Atoms., 467*, 146–151 https://doi.org/. 10.1016/J.NIMB.2019.11.047.

Mekhaldi, F., Czymzik, M., Adolphi, F., Sjolte, J., Björck, S., & Aldahan, A. (2020). Radionuclide wiggle matching reveals a nonsynchronous early Holocene climate oscillation in Greenland and western Europe around a grand solar minimum. *Climate of the Past., 16*, 1145–1157 https://doi.org/. 10.5194/cp-16-1145-2020.

Montgomery, D. C., & Runger, G. C. (2018). *Applied statistics and probability for engineers* (7th ed.). John Wiley & Sons, Inc..

Muscheler, R., Adolphi, F., Herbst, K., & Nilsson, A. (2016). The revised sunspot record

in comparison to cosmogenic radionuclide-based solar activity reconstructions. *Solar Physics, 291*, 3025–3043 https://doi.org/. 10.1007/s11207-016-0969-z.

Muscheler, R., Joos, F., Beer, J., Müller, S. A., Vonmoos, M., & Snowball, I. (2007). Solar activity during the last 1000 yr inferred from radionuclide records. *Quaternary Science Reviews, 26*, 82–97 https://doi.org/. 10.1016/j.quascirev.2006.07.012.

Parrenin, F., Barnola, J., Beer, J., Blunier, T., Castellano, E., & Chappellaz, J. (2007). The EDC3 chronology for the EPICA Dome C ice core. *Climate of the Past, 3*, 485–497. www.clim-past.net/3/485/2007/. (accessed April 22, 2021).

Pedro, J., van Ommen, T., Curran, M., Morgan, V., Smith, A., & McMorrow, A. (2006). Evidence for climate modulation of the 10Be solar activity proxy. *Journal of Geophysical Research, [Atmospheres]*, 111 https://doi.org/. 10.1029/2005JD006764.

Pedro, J. B., Heikkilä, U. E., Klekociuk, A., Smith, A. M., Van Ommen, T. D., & Curran, M. A. J. (2011). Beryllium-10 transport to Antarctica: Results from seasonally resolved observations and modeling. *Journal of Geophysical Research, [Atmospheres]*, 116 https://doi.org/. 10.1029/2011JD016530.

Pedro, J. B., McConnell, J. R., van Ommen, T. D., Fink, D., Curran, M. A. J., & Smith, A. M. (2012). Solar and climate influences on ice core 10Be records from Antarctica and Greenland during the neutron monitor era. *Earth and Planetary Science Letters, 355–356*, 174–186 https://doi.org/. 10.1016/j.epsl.2012.08.038.

Raisbeck, G. M., Yiou, F., Cattani, O., & Jouzel, J. (2006). 10Be evidence for the Matuyama-Brunhes geomagnetic reversal in the EPICA Dome C ice core. *Nature, 444*, 82–84 https://doi.org/. 10.1038/nature05266.

Raisbeck, G. M., Yiou, F., Jouzel, J., & Petit, J. R. (1990). 10 Be and δ 2 H in polar ice cores as a probe of the solar variability's influence on climate. *Philosophical Transactions of the Royal Society of London. Series A, Mathematical and Physical Sciences, 330*, 463–470 https://doi.org/. 10.1098/rsta.1990.0027.

Reimer, P. J., Austin, W. E. N., Bard, E., Bayliss, A., Blackwell, P. G., & Bronk, C. (2020). The IntCal20 northern hemisphere radiocarbon age calibration curve (0–55 cal kBP). *Radiocarbon, 62*, 725–757 https://doi.org/. 10.1017/RDC.2020.41.

Rix, J., Mulvaney, R., Hong, J., & Ashurst, D. A. N. (2019). Development of the British Antarctic survey rapid access isotope drill. *Journal of Glaciology, 65*, 288–298 https://doi.org/. 10.1017/jog.2019.9.

Siegenthaler, U. (1983). Uptake of excess CO_2 by an outcrop-diffusion model of the ocean. *Journal of Geophysical Research, 88*, 3599–3608 https://doi.org/. 10.1029/JC088iC06p03599.

Ståhle, L., & Wold, S. (1989). Analysis of variance (ANOVA). *Chemometrics and Intelligent Laboratory Systems, 6*, 259–272 https://doi.org/. 10.1016/0169-7439(89)80095-4.

Svalgaard, L., & Schatten, K. H. (2016). Reconstruction of the sunspot group number: the backbone method. *Solar Physics, 291*, 2653–2684 https://doi.org/. 10.1007/s11207-015-0815-8.

Synal, H. A. (2013). Developments in accelerator mass spectrometry. *International Journal of Mass Spectrometry, 349–350*, 192–202 https://doi.org/. 10.1016/j.ijms.2013.05.008.

Tiessen, C., Bemmerer, D., Rugel, G., Querfeld, R., Scharf, A., & Steinhauser, G. (2019). Accelerator mass spectrometry (AMS) for beryllium-7 measurements in smallest rainwater samples. *Journal of Radioanalytical and Nuclear Chemistry, 319*, 965–973 https://doi.org/. 10.1007/s10967-018-6371-6.

Vonmoos, M., Beer, J., & Muscheler, R. (2006). Large variations in Holocene solar activity: Constraints from 10Be in the Greenland ice core project ice core. *Journal of Geophysical Research: Space Physics, 111*, A10105 https://doi.org/. 10.1029/2005JA011500.

Yiou, F., Raisbeck, G. M., Baumgartner, S., Beer, J., Hammer, C., & Johnsen, S. (1997). Beryllium 10 in the Greenland ice core project ice core at summit, Greenland. *Journal of Geophysics Research: Ocean., 102*, 26783–26794 https://doi.org/. 10.1029/97JC01265.

Zheng, M., Adolphi, F., Sjolte, J., Aldahan, A., Possnert, G., & Wu, M. (2020). Solar and climate signals revealed by seasonal 10Be data from the NEEM ice core project for the neutron monitor period. *Earth and Planetary Science Letters, 541*, Article 116273 https://doi.org/. 10.1016/j.epsl.2020.116273.

Zheng, M., Sturevik-Storm, A., Nilsson, A., Adolphi, F., Aldahan, A., Possnert, G., & Muscheler, R. (2021). Geomagnetic dipole moment variations for the last glacial period inferred from cosmogenic radionuclides in Greenland ice cores via disentangling the climate and production signals. *Quaternary Science Reviews, 258*, Article 106881 https://doi.org/. 10.1016/j.quascirev.2021.106881.

L. Zipf, S. Merchel, P. Bohleber, G. Rugel, A. Scharf, Exploring ice core drilling chips from a cold Alpine glacier for cosmogenic radionuclide (10Be) analysis, Results Phys. 6 (2016) 78–79. https://doi.org/ 10.1016/j.rinp.2016.01.002.